Facile Exchange of Ligands on the 6-Mercaptopurine-Monolayer Protected Gold Clusters Surface†

ARTICLE *in* THE JOURNAL OF PHYSICAL CHEMISTRY C · MARCH 2010

Impact Factor: 4.77 · DOI: 10.1021/jp9122387

Facile Exchange of Ligands on the 6-Mercaptopurine-Monolayer Protected Gold Clusters Surface†

Encarnación Reyes, Rafael Madueño, Manuel Blázquez, and Teresa Pineda*

Departamento de Química Física y Termodinámica Aplicada, Universidad de Córdoba, Campus de Rabanales, Ed. Marie Curie, E-14071 Córdoba, Spain

Received: December 29, 2009; Revised Manuscript Received: February 17, 2010

We have investigated the exchange of 6-mercaptopurine (6MP) molecules by 11-mercaptoundecanoic acid (MUA) and 11-mercapto-1-undecanol (MUOH) on the surface of monolayer protected gold clusters (6MP-MPCs) of 2.4 nm diameter. After the addition of MUA or MUOH to the 6MP-MPC solutions the absorption band at 312 nm due to 6MP is suddenly observed. The monitoring of this signal allows us the study of the place-exchange reactions. The final products obtained from the exchange at different molecular ratios are characterized by IR spectroscopy. On the other hand, the ligand exchange reaction is slowed down upon increase nanoparticle size (6MP-AuNPs of 13 nm diameter) and, as expected, in two-dimensional surfaces (either 2D-polyfaceted or 2D-single crystal surfaces). Thus, it is concluded that the presence of defects in the monolayer due to the existence of a high ratio of edge and corner sites make easier the exchange of the 6MP by MUA or MUOH molecules being extremely difficult the exchange from the terraces that allow the organization of the molecules in the monolayer through lateral intermolecular interactions. Finally, the study of exchange in 2D-surfaces by means of electrochemical techniques evidence the important role of the stability of binding on the exchange kinetics.

Introduction

Ligand exchange reactions have become a particularly powerful approach to incorporate functionality in the ligand shell of thiol-stabilized nanoparticles and are widely used to produce organic- and water-soluble nanoparticles with various core sizes and functional groups.[1] The ligand shell composition allows one to tailor chemical properties such as solubility, chemical reactivity, surface chemistry, and binding affinity. To provide tailored nanoparticle samples for a wide range of applications, any synthetic method must be convenient and general, in addition to providing nanoparticles with well-defined structures. The control of the core size and composition is achieved through the careful choice of the reaction conditions during the synthesis or by postsynthetic modifications.[2]

In most cases, the gold nanoparticles are synthesized using the Brust method[3,4] or a variation of this method and are subsequently functionalized with other different thiolated surfactants than those used during synthesis by a ligand exchange process. Typically, in the place-exchange approach some foreign ligands are added to the as-synthesized nanoparticle solution and the mixture is allowed to react. Even though the ligand exchange reactions have shown great success in producing functional nanoparticles, the method requires a long time[5–7] and the complete exchange of the original ligand has not been demonstrated. However, the ligand exchange reaction is an extremely versatile tool for the preparation of functionalized metal nanoparticles with results that are fast and simple and allows the introduction of functional groups that are incompatible with other methods for nanoparticle synthesis.[8] It has been found[9] that the aging of the nanoparticles either during their synthesis or sample preparation has a profound impact on their reactivity, the freshly prepared ones being up to 10 times faster than the solutions aged for 1 week. It is concluded that this effect is due to the reorganization of the ligand shell on the surface. When the number of exchangeable sites per nanoparticle is very small (3−5 ligand per particle), these are likely defect sites rather than regular geometric features of a faceted nanoparticle (e.g., vertex or edge sites). The decreased reactivity of aged nanoparticles can thus be explained by annealing or stabilization of the high energy defect sites on the nanoparticle surface.

The research efforts of different groups to unravel the mechanisms of ligand exchange reactions have been recently reviewed,[10] emphasizing the control of the composition of the organic layer on the nanoparticle surface that can be reached by means of these reactions. The method is particularly useful for preparing nanoparticles functionalized with several different ligands.

Detailed studies on ligand exchange reactions in gold nanoparticles have revealed that the reaction is first-order with respect to the concentrations of both reagents, that is, the nanoparticles and the thiol, leading to the suggestion of an SN_2-type associative mechanism.[8,11] The population of different ligands in mixed monolayer nanoparticles that are produced by exchange reactions have been often determined by NMR,[12] IR spectroscopy,[13] and gas−liquid chromatography,[7] yielding the average number of ligands present per nanoparticle. Likewise, the kinetics have been followed by NMR[5,6,8,14] and gas−liquid chromatography[7] and have focused on the earliest stages of the reaction. Ligand exchange reactions of $Au_{25}(SCH_2CH_2Ph)_{18}$ with hexanethiol (HSC_6) and thiophenol (HSPh) as incoming ligands produce nanoparticles, having different relative populations of the two thiolate ligands that can be partially or almost completely exchanged depending on the reactant concentrations and the time of reactions as has been determined by matrix-

† Part of the special issue "Protected Metallic Clusters, Quantum Wells, and Metallic Nanocrystal Molecules".

* To whom correspondence should be addressed. E-mail: tpineda@uco.es. Phone: +34-957-218646. Fax: +34-957-218618.

10.1021/jp9122387
Published on Web 03/04/2010

assisted laser desorption ionization-time-of-flight (MALDI-TOF) mass spectrometric examination. Under the assumption that the reactivity of the 18 ligand sites are identical and independent, the equilibrium distributions of ligand populations of the mixed monolayer exchange products have been shown to adhere to a binomial distribution.[15] A comparison of the kinetics of exchanges of PhC_2S ligands of the MPCs $Au_{38}(SC_2Ph)_{24}$ and $Au_{140}(SC_2Ph)_{53}$ with p-substituted arylthiols allows to conclude that the first-order rate constants for the exchange of the first ca. 25% of the ligands vary linearly with the incoming arylthiol concentration. The ligand exchange is an overall second-order reaction and, remarkably, the second-order rate constants are very similar for the two sizes studied. The reason is that the locus of the initial ligand exchange is a common kind of site, thought to be the nanocrystal vertexes. The rates of later stages of exchange differ for different sizes, being much slower for the Au_{144}, presumably due to its larger terrace-like surface atom content.[6]

Zerbetto et al.[16] studied the kinetics of place-exchange reactions of thiols on gold nanoparticles. They proposed the use of fluorescence spectroscopy for monitoring the process and found that the exchange of ligands is consistent with an associative exchange path and that the insertion of the incoming thiol in the preformed lattice weakens the interaction of several adsorbed molecules, resulting in the rearrangement of more than a single unit in the reaction rate-determining step. They found that the dependence of the exchange reaction depends on the concentration of the incoming thiol, as would be expected for an associative mechanism. The kinetics present two different slopes suggesting the existence of two pseudofirst order processes with different rates, indicating some degree of surface inhomogeneity, which makes some sites more easily exchangeable than others as has already been observed.[8]

On the other hand, weakly bound ligands (e.g., short-chains thiolates, amines, sulfides) can be partially replaced from the surface of gold nanoparticles by disulfides. The exchange reaction shows zeroth-order with respect to the adsorbing disulfide.[17] In a mechanistic study of the place-exchange reaction only a small number of binding sites at the gold surface (3−5%) are found to be active in exchange. Triphenylphosphine-protected particles, however, were more reactive. The kinetics of exchange at high conversions required at least two exponential functions for an adequate fit, suggesting the presence of several different types of binding sites on the Au surface with a different reactivity toward the exchange.[18]

The formation of gold nanoparticles when the reaction was done in the presence of alcohol- or acid- terminated thiol or disulfide ligands was not observed using the Brust method[3,4] of $NaBH_4$ reduction of gold salt,[19] since the reduction of functional groups can also take place. Thus, substantial efforts have been dedicated to functionalize gold nanoparticles with different ω-functionalized alkylthiols to improve their versatility for applications. In this sense, different approaches have been used to obtain thiol protected gold nanoparticles through ligand exchange reactions.[20–23]

Recently, a method of producing thiol-stabilized, nearly monodisperse ω-functionalized thiolate gold nanoparticles in a single step using 9-borabicyclo[3,3,1] nonane (9-BBN) as a reducing agent has been reported. The synthetic protocol based on this mild reducing agent provided the opportunity to directly functionalize AuNPs with a variety of thiolated ligands during the synthesis.[24]

The development of a convenient synthesis method of 6MP-MPCs of 2.4 nm diameter[25] has encouraged us in the study of the ligand exchange reactions of these nanoparticles. The presence of the 6MP layer on the gold nanocluster surface makes these MPCs soluble in aqueous solutions and other polar solvents. We take advantage of both the solubility in polar solvents and the high degree of monodispersity of these MPCs to carry out some ligand exchange experiments in order to obtain mixed ligand monolayer protected gold nanoclusters of some specific ligands such as MUA and MUOH. In this work, we report the ligand exchange of the 6MP molecules of the 6MP-MPCs by both MUA or MUOH (Scheme 1) molecules and the easy quantification of the exchange processes by UV−visible spectroscopy. The exchange reaction is evidenced by IR spectroscopy. A comparison of the exchange reaction either in the MPCs or in a macroscopic 2D-surface (a polyfaceted gold electrode) is also reported.

SCHEME 1: Molecular Structure of the Ligand Molecules

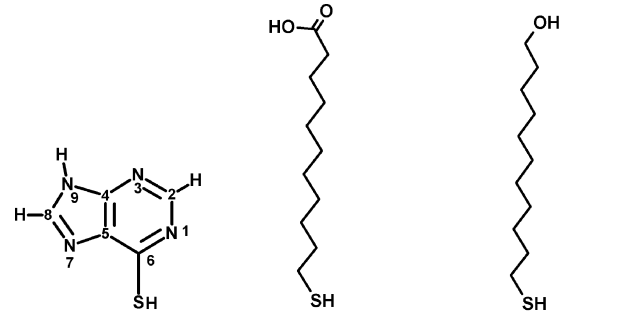

6-mercaptopurine **(6MP)** | 11-mercaptoundecanoic acid **(MUA)** | 11-mercapto-1-undecanol **(MUOH)**

Experimental Section

Chemical. 6-Mercaptopurine (6MP), 11-mercaptoundecanoic acid (MUA), and 11-mercapto-1-undecanol (MUOH), and semiconductor grade purity potassium hydroxide were purchased from Aldrich-Sigma. Hydrogen tetrachloroaurate trihydrate (from 99.999% pure gold) was prepared using a literature procedure[26] and stored in a freezer at −20 °C. All solutions were prepared with deionized water produced by Millipore system.

Synthesis of 6MP-MPCs. The synthesis of 6MP-MPCs was made by following a variation of the single phase system first derived by Brust el al.[4] by mixing 6MP (1.2 mmol in 10 mL DMF) with $HAuCl_4$ (0.3 mmol in 6 mL H_2O) under strong stirring conditions at a temperature of 4 °C. The solution turns red and later becomes colorless. After 30 min, sodium borohydride (3 mmol) was fastly added. The reaction mixture changes rapidly to black and then is left under stirring conditions for 1 h. All the process is carried out at a constant temperature of 4 °C. In order to eliminate the excess of 6MP molecules as well as other impurities, the solution containing all the reaction components was dialyzed against a 10 mM NaOH solution by using Spectra/Por dialysis tubes (MW range of 10.000). The dialysis was repeated up to the complete elimination of free 6MP molecules of the sample. The cleaning procedure was followed by UV−visible spectroscopy of the dialysis solution and finally by measuring the UV−visible spectrum of the 6MP-MPC sample.

Synthesis of 6MP-AuNPs. The synthesis of gold nanoparticles (AuNPs) has been carried out by following the classic method of Turkevitch et al.[27] that consists of the reduction of $HAuCl_4$ by citrate anions in an aqueous medium. The citrate

anions not only serve as a reductor agent, but they also exert a protection effect against the aggregation of the particles synthesized. Briefly, the gold nanoparticles were prepared as follows. In a 1-L Erlenmeyer flask, 500 mL of 1 mM $HAuCl_4$ was brought to a boil, with vigorous stirring on a magnetic stirring hot-plate. Fifty milliliters of 38.8 mM Na_3citrate was added to the solution all at once, with vigorous stirring. The yellow solution turned clear, dark blue, and then a deep red-burgundy color within a few minutes. Stirring and boiling was continued for 10−15 min after the burgundy color was observed. The solution was then removed from heat and kept stirring for 15 min. After the Au colloid solution had cooled, the volume was adjusted to 500 mL with H_2O. The modification of the AuNPs has been carried out by adding an excess of 6MP to the AuNPs aqueous solutions. Under these experimental conditions, only a slight change in the surface plasmon resonance (SPR) band of 3 nm after the modification is observed. The sample of 6MP-AuNPs was dialyzed against an aqueous solution to remove the 6MP molecules that have not reacted with the AuNPs. The formation of the 6MP-SAM on the AuNP surface has been demonstrated by FT-IR spectroscopy.[28]

Cyanide Decomposition Experiments. NaCN was added to the solutions containing the nanoparticles, and the absorbances at 400 and 520 nm for the 6MP-MPCs and 6MP-AuNPs, respectively, were recorded until the absorbance was low and constant. The spectra were recorded before and after NaCN was added.

Ligand Exchange Experiments. For the 6MP-MPCs, solutions of approximately 0.5 mg/mL in 10 mM NaOH were mixed with a *n*-fold ($n = 0.5$, 1, 2, and 10) molar excess (in reference to the MPC monolayer content) of MUA and were monitored by measuring the absorbance at 312 nm for the kinetics experiments or by recording spectra after the time to reach equilibrium. In the case of 6MP-AuNPs, solutions of 17 nM in AuNPs were used.

Methods

UV−Visible and Infrared Spectroscopies. UV−visible spectra were collected with a JASCO UV−visible−NIR (model V-570) spectrometer. Infrared measurements of solid samples (KBr) were conducted with a Bruker (mod. Alpha T) spectrometer.

Cyclic Voltammetry. A conventional three electrodes cell comprising a platinum coil as the counter electrode, a saturated calomel electrode as the reference electrode and a gold working electrode was used. The gold working electrodes were either a polyfaceted gold or a Au(111) single crystal. The polyfaceted gold electrode was a homemade sphere of approximately 3-mm diameter that was grown by melting a high purity Au wire (99.9998%) following the method developed by Clavilier.[29,30] Before each electrochemical measurement, the electrode was annealed in a natural gas flame to a light red melt for about 20 s and, after a short period of cooling in air, quenched in ultrapure water. The electrode was then transferred into the electrochemical cell with a droplet of water adhering to it to prevent contamination. The surface condition was confirmed by a cyclic voltammogram in 0.01 M $HClO_4$, and the real surface area was determined from the reduction peak of oxygen adsorption on the Au electrode. This surface treatment was the most appropriate to produce a surface that is clean, ordered and highly reproducible. The Au(111) single crystal electrode was a homemade hemisphere obtained by cutting and polishing an appropriately oriented sphere formed as explained above.

Cyclic voltammetry (CV) was recorded on an Autolab (Ecochemie model Pgstat20) instrument attached to a PC with proper software (GPES and FRA) for total control of the experiments and data acquisition.

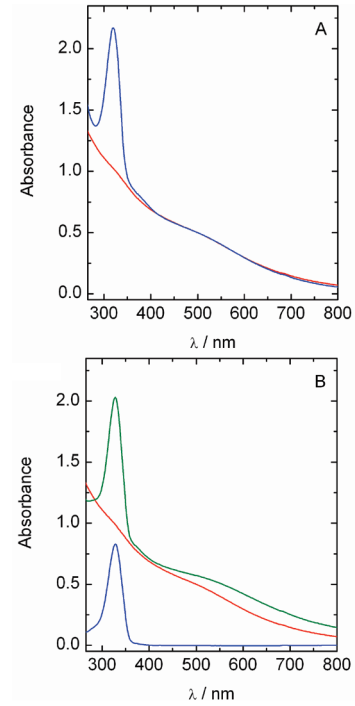

Figure 1. Ligand exchange reaction in 6MP-MPCs. UV−visible spectra of 4.65 μM 6MP-MPCs in: (A) (red line) 10 mM NaOH; (blue line) the mixture after 30 min of the addition of 10 mol equivalent MUA; (B) (red line) 10 mM NaOH; (green line) the mixture after 30 min of the addition of 10 mol equivalent MUA in acid medium; (blue line) supernatant after centrifugation of the mixture, in acid medium.

Results and Discussion

6-Mercaptopurine-Protected Gold Clusters (6MP-MPCs). Figure 1 shows the absorption spectra of 6MP-MPCs in 10 mM NaOH aqueous solution before and after 30 min of the addition of MUA. The spectrum of 6MP-MPCs shows a smooth band at 526 nm and a small shoulder at around 310−315 nm. The former band corresponds to the surface plasmon resonance transition, typical of this size of nanoclusters (2.4 ± 0.5 nm).[25] It is interesting to point out the almost inexistent signature due to the 6MP ligand at 315 nm that should be related to the interaction with the gold surface. It has been already described[31] that the absorption spectra of some dye molecules change upon binding to gold nanoparticle surfaces. In this study, the dye molecules have been classified into two classes, those that show an additive spectrum and those that bleach or reduce[32] in absorption intensity. The adsorbates belonging to the later class are the ones that interact electrostatically with the citrate layer of the nanoparticle with an orientation of the transition moment parallel to the surface.

However, in the case of the 6MP-MPCs used in the present work, the 6MP molecules are bound to the gold surface by the strong S−Au interaction, as has been shown by XPS, and are nearly perpendicular to the surface if we take into account the footprint area of the molecules.[25] Thus, a different reason needs to be found for the bleaching effect in the present case. In this sense, we can take into account the hypochromic effect shown by the nitrogen bases which is dependent upon the degree and orientation of intermolecular stacking interactions.[33]

The addition of a certain amount of MUA to the 6MP-MPCs solutions brings about an important change in the absorption

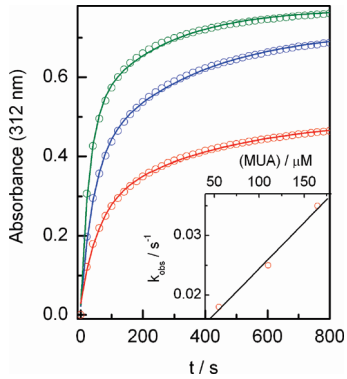

Figure 2. Ligand exchange kinetics of 6MP-MPCs monitored by UV−visible absorption spectroscopy. Evolution of the 312 nm band after the addition of (red line) 1 mol, (blue line) 2 mol, and (green line) 3 mol equivalent of MUA to 1 μM 6MP-MPCs in 10 mM NaOH. Solid lines are fits to biphasic pseudofirst order reaction (eq 1). Inset: Plot of the rate constant, k_{obs}, vs MUA concentration.

TABLE 1: Kinetic Results for MUA Ligand Exchange with 0.9 μM 6MP-MPCs

MUA/M ($\times 10^6$)	$[6MP]_{out}$/M ($\times 10^6$)[a]	A_1[b]	k_1/s^{-1} ($\times 10^2$)	A_2[b]	k_2/s^{-1} ($\times 10^3$)
55	27.2	0.22	1.8	0.21	2.44
110	39.4	0.33	2.5	0.30	2.96
165	42.0	0.43	3.5	0.25	4.10

[a] Concentration of 6MP liberated molecules upon the exchange reaction. [b] The values of the populations A_1 and A_2 are referred to the total amount of 6MP initially present on the MPCs surfaces.

spectrum. In fact, a strong absorption band at around 312 nm that coincides with that of 6MP in alkaline solution appears. In order to ascertain if the band corresponds to a surface bound or a solution chromophore, the pH of the solution was changed with the addition of perchloric acid to destabilize the dispersion and precipitate the MPCs. As can be seen (Figure 1B), the absorption band changes to 324 nm, in agreement with the behavior of 6MP in different pH aqueous solutions. Under these conditions, the surface plasmon resonance band of the MPCs shows an increased scatter at longer wavelengths indicating the loss of stability of the dispersion. The sample was then centrifuged and the supernatant gives the spectrum shown in Figure 1B. From these results, it can be concluded that the 6MP molecules are free in solution, and therefore, they have been displaced from the gold surface by the incoming ligand MUA. Thus, the absorption of the 6MP chromophore, which is bleached when bound to an MPC, is completely recovered after desorption from the gold surface. This interesting finding can be used to quantify the extent of ligand exchange and to follow the kinetics of the reaction.

The kinetic traces obtained for three different MUA concentrations are plotted in Figure 2. In order to find a good fitting of the data, two pseudofirst order processes have been supposed (eq 1):

$$A = A_1[1 - \exp(-\lambda_1 t)] + A_2[1 - \exp(-\lambda_2 t)] \quad (1)$$

where A_1 and A_2 are the contribution of the processes 1 and 2 and λ_1 and λ_2, the rate constants.

The extension of the ligand exchange reaction and the rate constant depend on the incoming ligand concentration (Table 1) but, in all cases, the reaction reaches equilibrium. The variation of the faster pseudofirst order rate constant with the incoming ligand concentration is linear (inset of Figure 2), although a fractional reaction order of 0.59 is obtained. This suggests that the insertion of a molecule of MUA weakens the interaction of more than a single 6MP unit, a fact that has been previously reported for the exchange of a pyrene-derivative by decanethiol on gold nanoparticle surfaces.[16] The partial absence of the initial π-stacking of the pyrene molecules upon exchange has been thought to be responsible for the involvement of more than one pyrene-labeled thiol in the rate-determining step.

The contribution of the two different regimes in the kinetic process are roughly similar at the lower MUA concentration but increases for the process taking place at a faster rate with increasing incoming ligand concentration. As the occurrence of a biphasic kinetics has been related with some degree of surface inhomogeneity,[8,16] this phenomenon should be related with the different surface sites on the nanoparticle surface which makes some sites more easily exchangeable than others.

The change of temperature in the range of 10 to 60 °C, at a ratio of MPC:MUA of 1:1, brings about an increase of the overall rate, although the traces continue showing biphasic behavior. However, it is found that the ratio of molecules exchanged in the first process increases from 0.45 at 10 °C up to 0.75 at the higher temperature studied with a parallel decrease of the population of the second process (see the Supporting Information).

The dynamics of ligand exchange in gold nanoparticles has been recently explained on the basis of the "hairy ball theorem" that states that it is not possible to align hairs into a sphere without generating two singularities that are called poles.[34,35] That is, the formation of a two-dimensional ordering is topologically possible only if two poles or defects are present at opposite ends of the nanoparticles. A recent molecular dynamics simulation study has evidenced that the molecules at the poles are weakly stabilized by their neighbors and should be the first molecules to be replaced in place-exchange reactions.[36] On the other hand, it has been found that the rate for exchange of the ligands at the poles is much higher than that at defects other than the poles, as these are thermodynamically distinct from those at crystallographically defined vertices of the core crystal.[34] By taking in mind these ideas, it can be concluded that the high exchange rate of the 6MP molecules from these clusters should be due to the destabilization of the molecules around the poles that should take place concomitantly with the loss of the stacking interactions. Moreover, the increase of the population of molecules exchanging by the faster process upon increasing temperature, should also be related to the lack of these stacking interactions under these conditions.

The exchange reaction has been carried out by using different 6MP:MUA ratios and, after the equilibrium is reached, the exchanged nanoclusters are cleaned by successive centrifugation and redisolution steps. This procedure involves the quantification of the 6MP molecules in the supernatants obtained in the different washing solutions. When the supernatant shows no signal of 6MP, the pellet containing the 6MP-MUA-MPCs is dried of solvent and examined by IR spectroscopy. The IR spectra of the 6MP-MUA-MPCs obtained after these exchange processes are plotted in Figure 3.

At the lower ratio employed (6MP:MUA of 1:0.5), the bands at 2849 and 2916 cm^{-1}, corresponding to the symmetric and asymmetric stretching vibrations, respectively, of the methylene groups of MUA appear. Moreover, as the ratio increases, the bands in the region of 1800 to 700 cm^{-1} of the 6MP disappear while this at 1720 cm^{-1} due to the carbonyl group at the

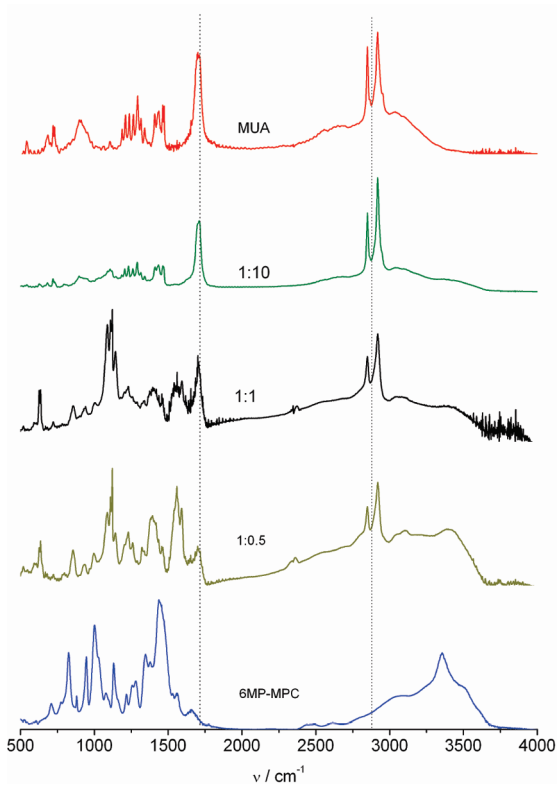

Figure 3. FT-IR spectra of the 6MP-MPCs and the products obtained after 0.5, 1, and 10 mol equivalent of MUA were mixed and the time for equilibrium was reached. The spectrum of free MUA is also shown for comparison.

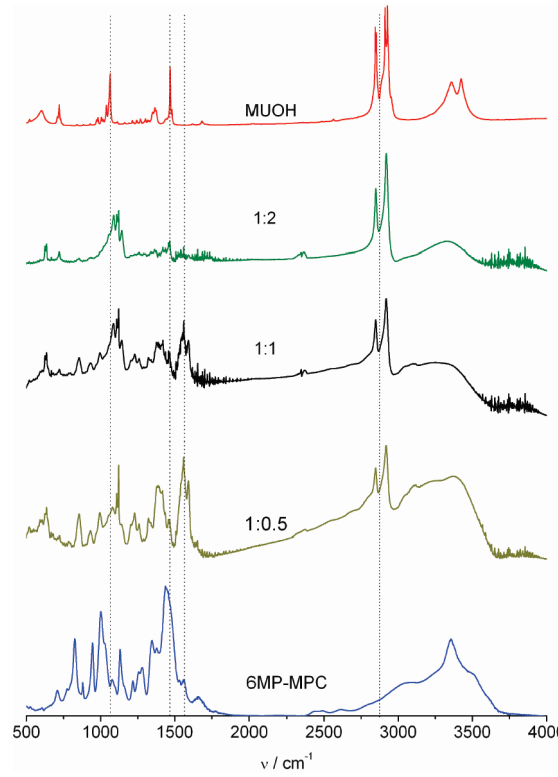

Figure 4. FT-IR spectra of the 6MP-MPCs and the products obtained after 0.5, 1, and 2 mol equivalent of MUOH were mixed and the time for equilibrium was reached. The spectrum of free MUOH is also shown for comparison.

ω-carboxyl terminal increases. At the molar ratio of 1:10, the spectrum resembles that of MUA and no residual bands of 6MP are visible.

The same exchange protocol has been used with MUOH in the place of MUA. Under these conditions, the exchange process is also very fast and shows a similar behavior to that of MUA. In Figure 4, the IR spectra of the 6MP-MUOH-MPCs obtained are shown. In a similar way that was observed for MUA, the exchanged products obtained at low ratio show the prominent bands at 2852 and 2922 cm^{-1} due to the symmetric and asymmetric stretching vibrations of the methylene groups of the MUOH molecules. Moreover, the spectral region of 500 to 1800 cm^{-1} become less crowded for the exchanged products up to the higher ratio where only the lines corresponding to MUOH are visible.

As has been pointed out above, the drastic change in absorbance for the 6MP molecules when going from the adsorbed to the solution state can be used to make a quantification of the extent of ligand exchange. As the 6MP-MPCs can be dried and redissolved without aggregation and taking advantage that the stoichiometry of these MPCs is known ($Au_{459}(6MP)_{62}$),[25] the quantification can be easily carried out. However, in order to better determine the fraction of 6MP exchanged we have carried out the etching of the 6MP-MPCs with CN anions to determine the total 6MP in the MPCs. The cyanide digestion of gold nanoparticles has recently been used to check the density and packing of the capping monolayer and the ligands ability to shield the gold core. In fact, when CN anions come into contact with the inorganic core, they form complexes with the gold atoms ($Au(CN)_2^-$), progressively etching the nanoparticle surface. In this sense, the NP resistance to NaCN digestion has been found to be affected by a combination of ligand footprint and packing density on the nanoparticle surface.[37]

The NaCN concentration used in the present experiment was chosen to be 3-fold over the number of gold atoms in the MPC sample.[25] We have monitored the etching process by following the changes in absorbance at 400 nm upon the addition of cyanide to the 6MP-MPCs solution (Figure 5A). After some time (~30 min), the reaction ends and the spectrum obtained shows (Figure 5B) the presence of 6MP (band at 312 nm) together with the signals corresponding to $Au(CN)_2^-$ (211, 230, and 240 nm).[11] Under these conditions, all the 6MP molecules that were bound to the nanoclusters surface are now free in solution. This measurements allows us to obtain the total amount of 6MP and, therefore, the stoichiometry of the 6MP-MPCs that agrees with that determined by TEM and thermogravimetric analysis measurements of $Au_{459}(6MP)_{62}$.[25] Taking in mind these results, we can determine the fraction of exchanged molecules in the experiments shown in Figures 3 and 4, resulting that approximately 100, 50 and 22% of 6MP molecules have been exchanged in the experiments in which 10, 1, and 0.5 fold of MUA, respectively, have been used. Although the method is somewhat rough, it can be said that, under the 10:1 ratio conditions, the 6MP molecules can be completely exchanged by MUA molecules on the 6MP-MPCs surface. This finding is very interesting as it has been reported that the complete exchange of ligands was not possible in the gold nanoparticles.[10] The exchange efficiency is of the same order for the MUOH molecules, being 98, 43 and 24%, for the 2, 1, and 0.5 fold of MUOH, respectively.

The most interesting findings in this ligand exchange procedure are on one hand, the complete substitution of the 6MP molecules at high molar ratios of the incoming ligand and, on the other hand, the fast reaction rate. In this sense, the time to

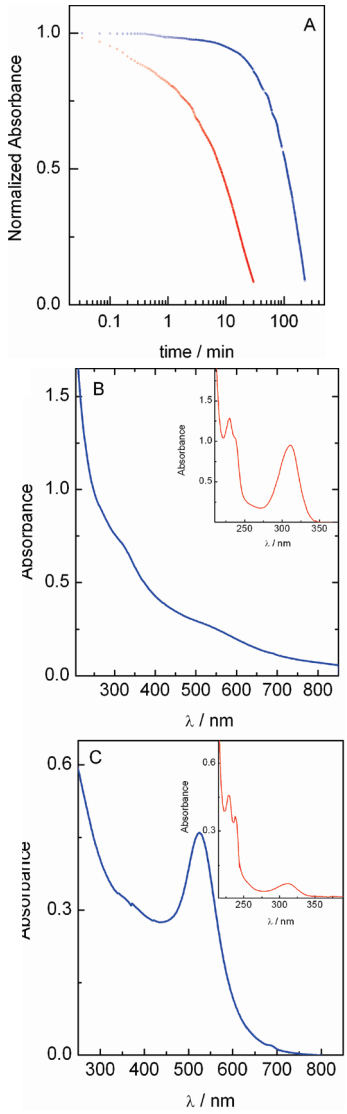

Figure 5. (A) Cyanide digestion of 6MP-MPCs (red line) and 6MP-AuNPs (blue line) (the experimental conditions are explained in the text); (B) UV−visible spectrum of the 6MP-MPCs. The inset shows the spectrum obtained for the same sample after cyanide digestion. (C) UV−visible spectrum of the 6MP-AuNPs. The inset shows the spectrum obtained for the same sample after cyanide digestion.

reach equilibrium is several orders of magnitude lower than those in other reported systems.[10] However, it is worth noting that in the latter cases, the incoming ligands have structures similar to those bound to the nanoparticle surface whereas in the present experiments, the incoming ligands possess different chemical and steric properties and, more importantly, different affinity for the gold surface (Scheme 1).

6MP-Gold Nanoparticles (6MP-AuNP) and Two-Dimensional 6MP-Self-Assembled Monolayers (2D-6MP-SAM). It is well-known that the dynamics of ligand exchange depends on the precise arrangement of the ligands on the nanoparticle surface, and the nature and accessibility of the Au sites.[10] Thus, if we take into account the surface area of the 6MP, the shape of the MPCs, and the number of surface atoms in terrace or edge sites,[38–40] we can think that the long-range stacking interactions[41–44] between 6MP molecules bound to the gold nanocluster become weaker than in the case of the 2D-6MP-SAM. In fact, the surface coverage for the 6MP-MPCs is higher than that for the 2D-6MP-MPCs in Au(111) single crystal surface[25,42] as has been found for alkanethiolate MPCs.[38,39,45] This fact has been explained as being due to the curvature of the nanoclusters that allows a better packing of the molecule chains with respect to flat gold surfaces. The consequence of this is the decrease of the ligand molecule footprint on going from 2D-SAM to MPCs. However, the effect of the curvature radius of the nanoclusters in the footprint of the 6MP[25] is smaller than that found for alkanethiolates.[38,39] The reason for this difference can be found in the larger molecular surface area of the 6MP that makes the accommodation of the molecules to form a compact layer more difficult. In fact, if we take into account the structure of the 6MP and the position of the thiol anchor group, the steric factor imposed by the imidazole ring is clearly evidenced. If the formation of hydrogen bonds between the different nitrogen groups in the purine rings of the adjacent 6MP molecules is assumed, a compact and stable layer around the gold nanocluster can be formed. This fact is reinforced by the additional interaction of the N(7) atom with the gold surface.[42] However, the efficient formation of hydrogen bonds needs a specific molecular arrangement in order to get the appropriate distance between the participating group that is not facilitated by the presence of edges and corners in the particle surface. Moreover, the interaction N(7)-Au can also be lost in these positions facilitating the mobility of the purine ring around the S−C(6) bond and creating holes that separate ordered patches. Therefore, the defects that can exist in these areas make it easy for the entrance of the MUA molecules that have a smaller footprint than the 6MP and stronger affinity for the gold surface as will be explained below.

In order to ascertain if the presence of these defects in the nanocluster protecting layer are responsible for the high degree and rate of ligand exchange, we have carried out a set of experiments by using larger nanoparticles protected by the same ligand such as the 6MP-AuNPs. These have been prepared by the modification of 13 nm citrate protected gold nanoparticles with 6MP upon the displacement of the citrate protective layer.[28] The exchange reaction in this case is very slow and the results difficult to follow with the chromophore displacement approach used for the smaller 6MP-MPCs (in the case of 6MP-AuNPs the strong plasmon absorption hamper the phenomenon). Moreover, by using the cyanide digestion method, it can be observed that the 6MP-AuNPs exhibit a slower digestion rate (Figure 5A), thus allowing us to conclude that these larger nanoparticles present a reduced defect area to be sampled due to the smaller surface curvature. In this way, the lateral interactions of the 6MP molecules can be stronger than in the 6MP-MPCs and, thus, a major resistance against ligand exchange is found.

In order to check this hypothesis, a study of the ligand exchange in the 2D-6MP-SAM has been carried out. While the 6MP-SAM built on a Au(111) single crystal electrode is maintained after more than 72 h in contact with a 1 mM MUA solution, the process is somewhat different when the gold substrate is a polyfaceted gold sphere. In this case, the electrode surface presents some well-defined facets that can be identified as the (111), (100), and (110), as well as other portions of the surface that cannot be ascribed to definite crystal planes and will be denominated as the polycrystalline surface. We address this problem by studying the reductive desorption process of the 6MP-SAM formed on the polyfaceted surface (Figure 6). This process has been characterized in our laboratory[44] and the peaks obtained in the cyclic voltammogram were ascribed to the different crystal facets, thus, the peaks at −0.7, −0.91, and −1.09 V correspond to the desorption of the 6MP molecules from the (111), (100), and (110) gold single crystal facets,

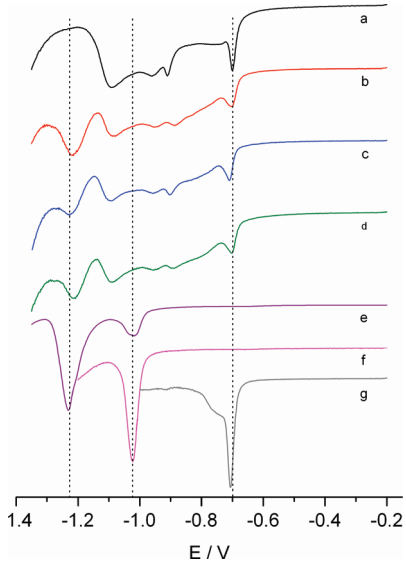

Figure 6. Voltammograms for the reductive desorption processes of (a) 6MP-SAM; 6MP-MUA-SAMs formed after contacting a 6MP-SAM with 1 mM MUA solution for (b) 15, (c) 30, and (d) 70 h; (e) voltammogram for the reductive desorption process of MUA-SAM. Voltammograms a−e were obtained by using a polyfaceted gold electrode. Reductive desorption processes of (f) MUA-SAM and (g) 6MP-SAM obtained by using a Au(111) single crystal electrode. The working solutions were 0.1 M KOH.

respectively. On the other hand, the reductive desorption process of the MUA-SAM on this polyfaceted electrode shows two peaks at −1.02 and −1.23 V (Figure 6e). By comparison with the same process carried out in an Au(111) single crystal electrode (Figure 6f), we assigned the first peak to the desorption from the (111) facets while the peak at more negative potentials to the rest of the surface. The voltammograms b−d in Figure 6 correspond to experiments in which the 6MP-SAM gold surface is in contact with 1 mM MUA solution for 15, 30, and 70 h, respectively.

There are two interesting features to highlight in the observed behavior. On one hand, the reduction peak at −0.7 V that corresponds to the desorption of the 6MP molecules from the (111) facets (see voltammogram (g) for comparison) remains in all cases and, on the other hand, only the peak at −1.23 V, corresponding to desorption of MUA from facets different from the (111), increases. Taking together these results, it can be concluded that the displacement of 6MP molecules by MUA from the Au(111) facets, where it is known that they form well organized structures with strong lateral interactions, is extremely difficult. However, the exchange is possible in the region where the gold surfaces are not well-defined and do not allow the long-range interactions of the 6MP molecules.

In this point, it is interesting to note that the different footprints of these molecules in 2D-surfaces are reflected in the charge density obtained for the reductive desorption of the two SAMs using the same polyfaceted gold substrate. Values of 56 and 67 μC/cm^2 are obtained for the 6MP- and MUA-SAM, respectively, indicating that the area occupied for MUA (23.9 Å^2) is lower than that for 6MP (28.6 Å^2). These results suggest that the number of incoming MUA molecules that adsorb in the gold surface are higher that the number of outgoing 6MP molecules. Although the determination of the charge density for desorption of the mixed layers is not accurate, this trend can be observed. This finding can be transferred to the MPCs and then, it can be established that, although the chromophore displacement method allows us to determine the amount of 6MP molecules that desorbs from the nanocluster surface, the number of MUA molecules that replaces them is higher than this figure although it is undefined.

Finally, it should be highlighted that the reductive desorption experiment for ligand exchange in 2D-surfaces gives us important information relative to the nature of the exchange process itself. It is well-known that the potential for the reductive desorption process is directly related to the SAM stability.[46,47] Thus, the high potential difference between the processes for the 6MP- and MUA-SAMs (∼300 mV for the reductive desorption from the Au(111) single crystal surfaces) indicates that the exchange process would be very efficient when the 6MP molecules are exchanged by MUA, but the reverse reaction would not succeed. In fact, the high rate of exchange observed for this reaction is a result of both the higher stability of the MUA-gold interaction that should increase the direct rate and the comparatively lower affinity of the 6MP for the gold, which should decrease the reverse rate constant.

Conclusions

The 6MP molecules are readily exchanged by MUA or MUOH molecules on the 6MP-MPC surface. The exchange reaction is monitored by UV−visible spectroscopy and the rate depends on the ratio of incoming ligand to nanocluster concentration. The kinetic traces are biphasic, in agreement with the lack of surface homogeneity, and the reaction reaches equilibrium. The 6MP-MUA- or 6MP-MUOH-MPCs obtained are characterized by infrared spectroscopy, and it is demonstrated that the 6MP molecules are completely exchanged on the 6MP-MPC surface at high concentration of the incoming ligand.

The rate of reaction decreases as the size of the gold cluster increases. Hence, the behavior on the ligand exchange dynamics in the limit of 2D-gold surface as studied in Au(111) single crystal and Au-polyfaceted surfaces is also in agreement. Although the 6MP molecules in the 6MP-SAM-Au(111) surface are not exchanged, those in the 6MP-SAM-polyfaceted gold show a moderate tendency to substitution. In fact, those 6MP molecules bound to the (111)-terraces where they form well organized structures with strong lateral interactions are not exchanged.

The different chemical and steric properties of the incoming ligands in comparison to the 6MP molecules in addition to the different affinity for the gold surface are thought to be the reasons for the fast and complete place-exchange reaction. However, the high ratio of surface atoms in edge and corner sites in the smaller clusters in comparison to the bigger ones provokes the existence of defects in the protective monolayers that should be responsible for the facile entrance of the incoming molecules and the displacement of the poorly bound ligands. An alternative explanation can be given by taking into account the hairy ball theorem. Thus, it is worth mentioning that the formation of polar defects has been found to occur in the size range from ∼2.5 to ∼8.0 nm.[48] In this sense, although the 6MP-MPCs are in the low limit of sizes, it can be concluded that the ligand exchange should start at the more reactive polar sites and continue by the destabilization of the molecules around these sites probably caused by the loss of stacking interactions between the purine rings when the 6MP molecules are replaced by MUA.

Acknowledgment. We thank the Ministerio de Ciencia e Innovación (MICINN) (Project CTQ2007-62723/BQU) Junta de Andalucía and University of Córdoba for financial support of this work.

Supporting Information Available: Additional Figures. This material is available free of charge via the Internet at http://pubs.acs.org.

References and Notes

(1) Warner, M. G.; Hutchison, J. E. *Functionalization and Surface Treatment of Nanoparticles*; American Scientific Publishers: San Francisco, 2003.
(2) Woehrle, G. H.; Brown, L. O.; Hutchison, J. E. *J. Am. Chem. Soc.* **2005**, *127*, 2172.
(3) Brust, M.; Walker, M.; Bethell, D.; Schiffrin, D. J.; Whyman, R. *J. Chem. Soc. Chem. Commun.* **1994**, 801.
(4) Brust, M.; Fink, J.; Bethell, D.; Schiffrin, D. J.; Kiely, C. *J. Chem. Soc. Chem. Commun.* **1995**, 1655.
(5) Song, Y.; Murray, R. W. *J. Am. Chem. Soc.* **2002**, *124*, 7096.
(6) Guo, R.; Song, Y.; Wang, G. L.; Murray, R. W. *J. Am. Chem. Soc.* **2005**, *127*, 2752.
(7) Kassam, A.; Bremner, G.; Clark, B.; Ulibarri, G.; Lennox, R. B. *J. Am. Chem. Soc.* **2006**, *128*, 3476.
(8) Hostetler, M. J.; Templeton, A. C.; Murray, R. W. *Langmuir* **1999**, *15*, 3782.
(9) Song, Y.; Huang, T.; Murray, R. W. *J. Am. Chem. Soc.* **2003**, *125*, 11694.
(10) Caragheorgheopol, A.; Chechik, V. *Phys. Chem. Chem. Phys.* **2008**, *10*, 5029.
(11) Templeton, A. C.; Wuelfing, M. P.; Murray, R. W. *Acc. Chem. Res.* **2000**, *33*, 27.
(12) Templeton, A. C.; Hostetler, M. J.; Warmoth, E. K.; Chen, S. W.; Hartshorn, C. M.; Krishnamurthy, V. M.; Forbes, M. D. E.; Murray, R. W. *J. Am. Chem. Soc.* **1998**, *120*, 4845.
(13) Jackson, A. M.; Myerson, J. W.; Stellacci, F. *Nat. Mater.* **2004**, *3*, 330.
(14) Donkers, R. L.; Song, Y.; Murray, R. W. *Langmuir* **2004**, *20*, 4703.
(15) Dass, A.; Holt, K.; Parker, J. F.; Feldberg, S. W.; Murray, R. W. *J. Phys. Chem. C* **2008**, *112*, 20276.
(16) Montalti, M.; Prodi, L.; Zaccheroni, N.; Baxter, R.; Teobaldi, G.; Zerbetto, F. *Langmuir* **2003**, *19*, 5172.
(17) Ionita, P.; Caragheorgheopol, A.; Gilbert, B. C.; Chechik, V. *J. Am. Chem. Soc.* **2002**, *124*, 9048.
(18) Ionita, P.; Caragheorgheopol, A.; Gilbert, B. C.; Chechik, V. *Langmuir* **2004**, *20*, 11536.
(19) Roth, P. J.; Theato, P. *Chem. Mater.* **2008**, *20*, 1614.
(20) Brown, L. O.; Hutchison, J. E. *J. Am. Chem. Soc.* **1999**, *121*, 882.
(21) Brown, L. O.; Hutchison, J. E. *J. Am. Chem. Soc.* **1997**, *119*, 12384.
(22) Wang, G. L.; Huang, T.; Murray, R. W.; Menard, L.; Nuzzo, R. G. *J. Am. Chem. Soc.* **2005**, *127*, 812.
(23) Hong, R.; Emrick, T.; Rotello, V. M. *J. Am. Chem. Soc.* **2004**, *126*, 13572.
(24) Sardar, R.; Shumaker-Parry, J. S. *Chem. Mater.* **2009**, *21*, 1167.
(25) Viudez, A. J.; Madueno, R.; Blazquez, M.; Pineda, T. *J. Phys. Chem. C* **2009**, *113*, 5186.
(26) Brauer, G. *Handbook of Preparative Inorganic Chemistry*; Academic Press: New York, 1965.
(27) Turkevic, J.; Kim, G. *Science* **1970**, *169*, 873.
(28) Viudez, A. J.; Madueno, R.; Pineda, T.; Blazquez, M. *J. Phys. Chem. B* **2006**, *110*, 17840.
(29) Clavilier, J.; Armand, D.; Sun, S. G.; Petit, M. *J. Electroanal. Chem.* **1986**, *205*, 267.
(30) Clavilier, J.; Faure, R.; Guinet, G.; Durand, R. *J. Electroanal. Chem.* **1980**, *107*, 205.
(31) Franzen, S.; Folmer, J. C. W.; Glomm, W. R.; O'Neal, R. *J. Phys. Chem. A* **2002**, *106*, 6533.
(32) Battistini, G.; Cozzi, P. G.; Jalkanen, J. P.; Montalti, M.; Prodi, L.; Zaccheroni, N.; Zerbetto, F. *ACS Nano* **2008**, *2*, 77.
(33) Cantor, C. R.; Schimel, P. R. *Biophysical Chemistry. The conformation of biological macromolecules*; W. H. Freeman and Co.: New York, 1980; Vol. I.
(34) DeVries, G. A.; Brunnbauer, M.; Hu, Y.; Jackson, A. M.; Long, B.; Neltner, B. T.; Uzun, O.; Wunsch, B. H.; Stellacci, F. *Science* **2007**, *315*, 358.
(35) DeVries, G. A.; Talley, F. R.; Carney, R. P.; Stellacci, F. *Adv. Mater.* **2008**, *20*, 4243.
(36) Rapino, S.; Zerbetto, F. *Small* **2007**, *3*, 386.
(37) Mei, B. C.; Oh, E.; Susumu, K.; Farrell, D.; Mountziaris, T. J.; Mattoussi, H. *Langmuir* **2009**, *25*, 10604.
(38) Terrill, R. H.; Postlethwaite, T. A.; Chen, C. H.; Poon, C. D.; Terzis, A.; Chen, A. D.; Hutchison, J. E.; Clark, M. R.; Wignall, G.; Londono, J. D.; Superfine, R.; Falvo, M.; Johnson, C. S.; Samulski, E. T.; Murray, R. W. *J. Am. Chem. Soc.* **1995**, *117*, 12537.
(39) Hostetler, M. J.; Wingate, J. E.; Zhong, C. J.; Harris, J. E.; Vachet, R. W.; Clark, M. R.; Londono, J. D.; Green, S. J.; Stokes, J. J.; Wignall, G. D.; Glish, G. L.; Porter, M. D.; Evans, N. D.; Murray, R. W. *Langmuir* **1998**, *14*, 17.
(40) Whetten, R. L.; Khoury, J. T.; Alvarez, M. M.; Murthy, S.; Vezmar, I.; Wang, Z. L.; Stephens, P. W.; Cleveland, C. L.; Luedtke, W. D.; Landman, U. *Adv. Mater.* **1996**, *8*, 428.
(41) Madueno, R.; Garcia-Raya, D.; Viudez, A. J.; Sevilla, J. M.; Pineda, T.; Blazquez, M. *Langmuir* **2007**, *23*, 11027.
(42) Madueno, R.; Pineda, T.; Sevilla, J. M.; Blazquez, M. *Langmuir* **2002**, *18*, 3903.
(43) Madueno, R.; Pineda, T.; Sevilla, J. M.; Blazquez, M. *J. Phys. Chem. B* **2005**, *109*, 1491.
(44) Madueno, R.; Sevilla, J. M.; Pineda, T.; Roman, A. J.; Blazquez, M. *J. Electroanal. Chem.* **2001**, *506*, 92.
(45) Fabris, L.; Antonello, S.; Armelao, L.; Donkers, R. L.; Polo, F.; Toniolo, C.; Maran, F. *J. Am. Chem. Soc.* **2006**, *128*, 326.
(46) Hatchett, D. W.; Uibel, R. H.; Stevenson, K. J.; Harris, J. M.; White, H. S. *J. Am. Chem. Soc.* **1998**, *120*, 1062.
(47) Vela, M. E.; Martin, H.; Vericat, C.; Andreasen, G.; Creus, A. H.; Salvarezza, R. C. *J. Phys. Chem. B* **2000**, *104*, 11878.
(48) Carney, R. P.; DeVries, G. A.; Dubois, C.; Kim, H.; Kim, J. Y.; Singh, C.; Ghorai, P. K.; Tracy, J. B.; Stiles, R. L.; Murray, R. W.; Glotzer, S. C.; Stellacci, F. *J. Am. Chem. Soc.* **2008**, *130*, 798.

JP9122387